Chemical Papers (2021) 75:89–97
https://doi.org/10.1007/s11696-020-01282-3

ORIGINAL PAPER

An ellipsometric biosensor using aptamer for the detection of mercuric ions

Tuğçe Ertan[1] · Mustafa Oğuzhan Caglayan[1,2]

Received: 27 April 2020 / Accepted: 6 July 2020 / Published online: 14 July 2020

Abstract

An ellipsometric biosensor, to be used in the detection of mercuric ions that affect the vital organs of living organisms, was developed. In this context, as a diagnostic element of the developed ellipsometric biosensor, a nucleic acid-based aptamer that is highly selective for mercuric ions (Hg^{2+}) was used. Two different aptamers, a long and straight sequence, and a hairpin-structured oligonucleotide sequence were chosen. The detection sensitivity obtained by both aptamers was 0.237°/µM and 0.211°/µM, respectively. The detection limit was 0.89 pM $Hg^{2+}$and 187 nM Hg^{2+} for linear- and hairpin-type oligonucleotide, respectively.

Keywords DNA aptamer · Ellipsometry · Biosensor · Mercuric ion

Introduction

Mercuric ion (Hg^{2+}) is a common pollutant as one of the most important, stable, and water-soluble heavy metal ions in biological and environmental conditions (Liu et al. 2010). Mercury is a neurotoxin known to cause damage to many systems and kidneys, including cardiovascular, respiratory, gastrointestinal, hematological, immune, and reproductive systems (Jiang et al. 2016). Mercury compounds are easily consumed by bacteria, plankton, fish, and other marine mammals and accumulate in the tissues of these creatures and are included in the food chain through the biological cycle (Clarkson et al. 2003). It is reported that 84% of fish in the world seas contain mercury well above the safe levels (Grisci et al. 2016). Various studies have shown that mercury levels in many aquatic species can cause cellular activity disruption, as well as energy metabolism and reproductive system problems (Clarkson and Magos 2006; Dragone et al. 2009; Fanous et al. 2008). Therefore, an effective and fast method is required for the detection of mercury ions, especially in aqueous environments and food sources (Liu et al. 2016). The US Environmental Protection Agency (EPA) has set the upper limit of Hg^{2+} in drinking water to be 2 ppb (10 nM) to protect the public health (Clarkson and Magos 2006).

Several analytical methods have been reported for the detection of Hg^{2+}, including atomic absorption and inductively coupled plasma/mass spectroscopy (Lech 2014) and high-performance liquid chromatography (Bacon et al. 2020; Narukawa et al. 2018). Despite the full and rapid analysis capabilities of some of these official methods, each of these techniques has certain disadvantages such as requirements of chemistry and device knowledge, and sophisticated devices (Xiao et al. 2016). Alternatively, electrochemical, electromagnetic, and fluorescent methods have also been reported (Chamier and Crouch 2012; Chen et al. 2015; Dalmieda and Kruse 2019; Gabr and Christopher Pigge 2017; Jia et al. 2015; Li et al. 2009) (Zapata et al. 2010). Optical-based detection methods such as surface plasmon resonance (SPR) and ellipsometry, are preferred by some of the researchers since they offer several advantages, such as stability, reliability, and sensitivity (Chen and Wang 2020). There are studies on the SPR-based Hg^{2+} sensors that are using various recognition elements such as, 1,6-hexane dithiol (Chah et al. 2004), cross-linked chitosan (Fen et al. 2011), polypyrrole-chitosan polymer composite (Abdi et al. 2011), biotin-streptavidin conjugated gold nanoparticles (AuNPs) (Chao et al. 2012), and DNA aptamer conjugated AuNPs (Chang et al. 2011), in the literature.

✉ Mustafa Oğuzhan Caglayan
oguzhan.caglayan@bilecik.edu.tr

[1] Chemical Engineering Department, Sivas Cumhuriyet University, Sivas, Turkey

[2] Bioengineering Department, Bilecik Seyh Edebali University, Bilecik, Turkey

In the last 2 decades, spectrophotometric ellipsometry (SE) was a widely used and preferred method since film parameters, film thickness, composition, and optical properties of a thin film can be examined (Tompkins et al. 1998). The SE method measures the change in polarization when an electromagnetic wave is reflected from an interface. The determination of optical properties is generally carried out based on two or three-phase models (Bareiß et al. 2012). An important advantage of the ellipsometer is that it allows simultaneous control of surface quality, film thickness, and dielectric properties, especially during the growth of thin-film structures (Fang et al. 1996; Tompkins et al. 1998; Yim et al. 2014). The basic magnitude measured by an ellipsometer is the complex reflection rate which is a function of ellipsometric angles psi (Ψ) and delta (Δ). There are also sensor applications where ellipsometric approaches are used in combination with various recognition strategies (Arwin 2001; Caglayan and Üstündağ 2020; Jin et al. 2011; Wang et al. 2019).

In 1990, the two groups independently developed the in vitro selection and amplification of RNA sequences that can be specifically linked to target molecules (Ellington and Szostak 1990; Tuerk and Gold 1990). After the introduction of these functional RNA oligonucleotides, called aptamers (Jayasena 1999), DNA-based aptamers were also reported (Ellington and Szostak 1992). Especially with the development of fast and automated selection technologies, DNA and RNA aptamers have been selected in a wide target range (eg proteins, peptides, amino acids, drugs, metal ions, and even whole cells) (Ramos et al. 2007; Tombelli et al. 2007; Zhang et al. 2019). Aptamers derived from having the ability to fold after binding to the target molecule generally have a high affinity for the target molecules (Jayasena 1999). These aptamers can either be incorporated into small molecules in their nucleic acid structures or integrated into macromolecules such as proteins (Hermann and Patel 2000).

In this study, we report an ellipsometry-based aptasensor to detect Hg^{2+} in the aqueous media. Although SPR-based sensors and in some cases aptamer sequences were used for the detection of Hg^{2+} ions, especially ellipsometry and silicon substrate monolayer formations were not used together. For this purpose, to try to increase the detection limit, two different aptamer sequences, one in the linear and the other in hairpin structure, were used for the detection of Hg^{2+} using spectroscopic ellipsometry.

Experimental

In the first stage of the study, 3-Mercaptopropyltriethoxysilane (MPTES) was covalently attached to the surface of the Si wafer to form a self-assembled monolayer (SAM). During the modification process with MPTES, optimization of single-layer formation was performed. In the second stage of the study, the immobilization of two mercury-specific oligonucleotide probes (aptamers) on the MPTES substrate was optimized. At this stage, the aptamer probe was immobilized to the silicon wafer and a biochip chip was obtained. At the last stage, the evaluation of the mercury detection performance of biochip with spectroscopic ellipsometry (SE) was performed. Finally, mercury detection sensitivities and mercury detection limits (LOD) were evaluated and mercury sensing performances of two different aptamers were compared.

Chemicals and equipment

All chemicals used in this study are of an analytical or higher grade. Chemicals purchased were used as supplied without additional purification. Mercury-sensing aptamer probes were provided by Ella Biotech GmbH, Germany, in base sequence 5′-SH-AAA AAA AAA AAA AAA AAA AAT TCG TGT TGT GTT CG-3′ (Li et al. 2010) and 5′-SH-CGG GGG ACA GGA CTT GAC CTT CTC CGC CTT CTT CTC TCC TGT CCC CCG-3′, in quantities of 12.6 nmol and 11.4 nmol. Si wafers (100), on which the spectroscopic ellipsometry sensor surface is formed, were one side polished and in standard thickness. Absolute ethyl alcohol, 96% ethyl alcohol, and MPTES used in cleaning and modification of silicone surfaces were of high purity and purchased from Sigma-Aldrich. NaH_2PO_4, Na_2HPO_4, HCl, and NaOH were used to prepare the phosphate buffer solution. The mercury used in the test of the sensor was supplied by Sigma-Aldrich as mercury salt ($HgCl_2$). During the experiments, deionized water with a specific resistance of > 5 MΩ cm was used. Si-wafer surfaces were washed with high purity water and ethyl alcohol using an ultrasonic bath (JEIO TECH, Korea) before modification. The air and oxygen plasma system (Diener Electronics, USA) were used to clean the chemical impurities on the silicone surface and to form the oxide layer for modification.

Opt-S9000 ellipsometer device was used to measure the organic layer accumulation on the surface and the changes in the dielectric constants (i.e. Δ and Ψ) of the organic heavy metal complex (Caglayan et al. 2009; Demirel et al. 2007a, b). The ellipsometer device consists of two separate arms with a light source and detector and a goniometer where the angles of these arms are changed (Fig. 1). The polarized light is obtained from a monochromator unit, where the light from a polychromatic light source is reduced to a single wavelength. The light coming to the surface placed on the table at a certain angle from the light source then reflects from this surface and reaches the detector. The delta and psi angles (Δ and Ψ) are determined by measuring the change in the polarization states of the beam coming into the detector. The accumulation on the surface and surface roughness on

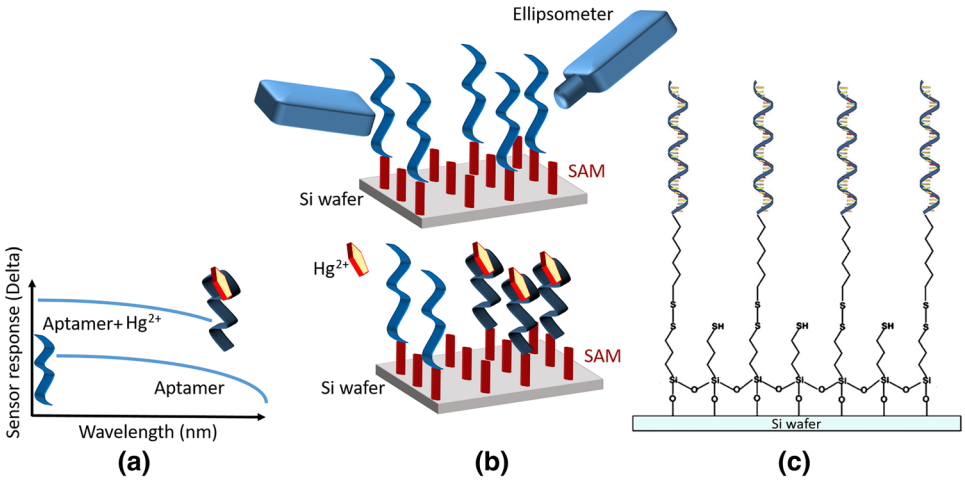

Fig. 1 Schematic representation of a typical sensor response (**a**), spectroscopic ellipsometry setup (**b**) and sensor surface, self-assembled layer and aptamers (**c**)

the prepared sensor surface was examined using the Park System XE 100 model atomic force microscope (AFM) in non-contact mode. Since the Si-wafer substrate is uniform and well crystalized, root-mean-square surface roughness data obtained using AFM can be used to compare surface deposition uniformity (Demirel et al. 2007b). All measurements were performed in an area of 5 µm × 5 µm using the NSC-15 model probe.

Otherwise stated, all data represented here were given as arithmetical mean of three replicates in series, and standard deviations were reported as 1σ of this data. The thickness and roughness data were collected using three specimens, and by measuring at least ten random points on a single specimen.

Modification of silicon wafer

Si wafers to be used were cut into 5 mm × 5 mm pieces using a diamond tip pen. The cut wafer pieces were cleaned in an ultrasonic bath for 10 min using 96% ethyl alcohol and then high purity water for 10 min. Si wafers were dried with nitrogen gas after bathing. After drying, it was kept in the plasma device for 20 min to remove organic impurities on the Si wafers and to form a hydroxylated surface for MPTES modification. The plasma device was operated at 100 W. The cleaned silicon surface was subjected to thickness measurement with an ellipsometer for control purposes.

In the modification made with MPTES, first, the duration of immersion was optimized. The MPTES solution was prepared in absolute ethyl alcohol (500 µM). As soon as the cleaned and hydroxylated Si wafers came out of the plasma device, a single layer was formed by immersing in 1 mL of MPTES solutions. With this process, a Si wafer surface functionalized with the thiol end group was obtained. Si wafers were kept in different durations (2, 3, 4, 6, and 24 h) in MPTES solution, in a light-free environment, and at room temperature. The Si wafers removed from the solution at the end of the specified periods were carefully washed with 96% ethyl alcohol and then dried with nitrogen gas. Dried samples were measured at an angle of 60° and 70° in the ellipsometer, in the wavelength range of 400–1700 nm. From the Δ and Ψ data obtained as a result of the measurement, the thickness of the organic layer was determined precisely by spectroscopic ellipsometry using a silicon substrate, SiO_2 layer and organic layer (with Cauchy model) as model parameters. Surface topography and roughness were obtained using AFM, then the optimum immersion time was determined and this period was used in all subsequent operations.

The optimum MPTES concentration was determined by changing the MPTES concentration in five different concentrations (500, 100, 50, 10, and 5 µM). After the Si wafers were cleaned using the processes described herein, they were immersed in 1 mL of MPTES solution. The Si wafers were kept in the light-free environment and at room temperature during the optimum period determined in the first experiment. After this period, the Si pieces removed from the solution were washed with 96% ethyl alcohol and then dried with nitrogen gas. In the same way, the established samples were analyzed with ellipsometer and AFM, and the optimum concentration for self-assembled layer formation was determined, and this determined concentration was used in all processes performed thereafter.

Oligonucleotide probe immobilization

The binding of thymine–Hg^{+2}–thymine (T–Hg^{+2}–T) for mercury ions is a selective form of binding. This selectivity was taken into account when selecting oligonucleotide probes. Oligonucleotide probes (aptamers) are available in different lengths and different structures. The aptamer sequences used are given in Table 1. While linear array was chosen as Prob1, hairpin structured oligonucleotide sequence was selected as Prob2. Mercury sensing –SH

Table 1 Aptamer sequences used in this study

Probe	Sequence	Circular structure calculated using mfold server (Zuker 2003)
Prob1	5′-SH-AAA AAA AAA AAA AAA AAA AAT TCG TGT TGT GTT CG-3’	Linear
Prob2	5′-SH-CGG GGG ACA GGA CTT GAC CTT CTC CGC CTT CTT CTC TCC TGT CCC CCG-3’	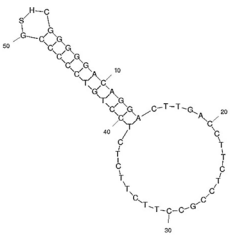
		ΔG = -8.27 kJ/mol

(thiol)-terminated aptamers were immobilized to MPTES-modified silicon surface according to the thiol–disulfide exchange reaction.

Experiments for the determination of optimum duration for immobilization were carried out using a 1 µM aptamer solution in 0.1 M pH 7.2 phosphate buffer (PBS). Self-assembled layers of MPTES-modified wafers were immersed in 1 mL of aptamer probe solution for 2, 4, 6, 12, and 24 h. The Si wafers removed from the solution at the end of these periods were washed with high purity water and then dried with nitrogen gas. Whether the optimum distribution of the aptamer probes on the surface is ensured or not was determined by ellipsometric thickness measurements. To determine the effect of concentration on the distribution of aptamer probes placed on the surface, the solution prepared in five different concentrations (1 µM, 500 nM, 100 nM, 50 nM, and 10 nM) was prepared in phosphate buffer solution (pH 7.2). The optimum time and concentration were determined by characterizing the dried samples with ellipsometer and AFM, and these optimum conditions were used in all processes performed thereafter.

Mercuric ion detection and sensor performance evaluation

The aptamer probe obtained is provided to interact with the immobilized sensor surface with mercury. Mercury, which is supplied in the form of mercury salt ($HgCl_2$), was diluted with water and a solution of 100 mM of mercury was prepared as a stock. The prepared silicon wafers were kept in 1 mL solution of 100 mM mercury solution for 6, 8. 12, 18, and 24 h. The Si wafers removed from the solution at the end of the specified period were washed with water and then dried with nitrogen gas. Optimum time was determined for mercury detection by analyzing the dried samples with an ellipsometer. Finally, the success of aptasensors as a Hg^{2+} sensor was checked by a spectroscopic ellipsometer. For this purpose, the sensor response was obtained by sending mercury at different concentrations on both aptasensors (Prob1 and Prob2). The silicon wafers prepared by the specified processes herein were immersed in 1 mL of solutions of 10 mM, 1 mM, 100 µM, 10 µM, 1 µM and 1 nM Hg^{2+} and kept for the time determined in the previous experiment. The Si wafers removed from the solution at the end of the period were washed with high purity water and then dried with nitrogen gas. By analyzing the dried samples with ellipsometers sensor detection limit (LOD) and detection sensitivity were determined and compared.

Results and discussion

Modification of silicon wafer and immobilization of probes

The immersion times have a great effect on the surface modifications of silane molecules. Si-wafer surfaces were modified with MPTES molecules for 2, 3, 4, 6, and 24 h. After ellipsometric measurements, the amount of MPTES molecules attached to the silicone surface was found as thickness by calculations made by the device’s modeling program. The calculated thicknesses for the 2, 3, 4, 6 and 24-h time intervals were determined as 0.43 ± 0.025, 0.87 ± 0.036, 1.36 ± 0.028, 1.82 ± 0.039 and 2.51 ± 0.0312 nm, respectively. In the first 4 h, single-layer formation was observed on the surface. However, the increase in thickness at longer immersion times shows that macromolecules are formed on the surface and multiple layers are not desired. The increase in thickness for long periods occurs as a result of the accumulation of MPTES molecules on the surface, possibly due to the ingress of water caused by the humidity of the air. It is likely that the moisture in the air is absorbed into ethyl alcohol and included in the reaction, especially in periods such as 24 h. Since the thickness of 1.36 nm formed at the

4th hour is suitable for the desired single-layer form, the immersion time was chosen as 4 h and this period was used in the later studies.

The effect of MPTES concentration on the thickness of the MPTES layer formed on the silicon surface and the formation structure were investigated. For this purpose, five different concentrations of MPTES/absolute ethyl alcohol solution (500, 100, 50, 10, and 5 µM) were used. The duration of immersion was 4 h which was determined in the previous section. The thicknesses at a concentration of 5 and 10 µM were determined as 1.22 ± 0.027 and 1.36 ± 0.027 nm, respectively. At the higher concentrations such as 100 µM, the thickness rose above 5 nm. The rapid thickness increase obtained at MPTES concentration of 100 µM and above indicates that there is physical accumulation. The structural formation that caused this thickness increase was examined using AFM. It was found that MPTES at a concentration of 10 µM with an RMS roughness of 1.41 ± 0.255 nm was suitable for the desired monolayer formation. In the immobilization process, the 5′-thiol-terminated oligonucleotide probes were covalently bound by MPTES directly by a disulfide bond. The structure formed on the sensor is shown schematically in Fig. 1.

In the optimum time determination study for immobilization of mercury-specific oligonucleotide probes, silicon wafers were kept in probe solution for 2, 4, 6, 12, and 24 h. The probe concentration used to determine the immobilization time is 1 µM and was prepared in 0.1 M pH 7.2 phosphate buffer solution. The immobilization of aptamer probes (Prob1 and Prob2) with disulfide bonds at different times was carried out at room temperature and in a light-free environment. In the optimization study, thicknesses were determined using a spectroscopic ellipsometer. Between 2 and 6 h, the thickness ranged from 1.35 to 1.87 nm, while at 12 h the thickness increased to around 2.71 ± 0.134 nm. No significant change in thickness was observed after 12 h, and, therefore, the time considered appropriate for probe immobilization was chosen as 12 h. Si wafers modified with MPTES were kept in probe solutions prepared in 5 different concentrations in the range of 1000–10 nM for 12 h. It was observed that the thickness at a concentration of 10 nM was 0.27 ± 0.123 nm, while the thickness at a concentration of 1 µM was up to 2.63 ± 0.111 nm. The immobilization of aptamer probes at a concentration of 1 µM for 12 h was determined as the optimum time and concentration during the preparation of the sensor chip.

Mercuric ion detection and sensor performance evaluation

Prob1 and Prob2 DNA oligonucleotides selected following T–Hg^{+2}–T binding for mercuric ions were immobilized separately to MPTES-modified silicone surface for 1 h at a concentration of 1 µM. In the time experiment with both probes, the levels of mercury were observed to be the same at all times, and it was determined that mercury detection was completed at the lowest time, 6 h. Two different sensors were obtained with this process, which was carried out using two oligonucleotide probes of different structure, and the sensor chip capacities of different diagnostic elements were evaluated.

The sensor chips obtained to determine the mercury detection limit and detection sensitivity have been tested in mercury solutions prepared at different concentrations. The phase shift (Δ) parameter was taken into account when evaluating the analyzes made with the ellipsometer device. The ellipsometric Δ parameter depends on the optical properties of the layers in which light is reflected, and, therefore, the complex diffraction index can be directly associated with the delta parameter. It is assumed that the reflection parameters for dielectric substances are directly dependent on the layer thickness for homogeneous layers (Poksinski and Arwin 2003). Also, since the Ψ angle, another ellipsometric data, is the ratio of light intensity between the polarization states of the reflected light, it is a kind of refractometric measurement and it is not sensitive to the targeted concentrations in this study. For the reasons stated, the change in the Δ parameter measured using a spectroscopic ellipsometer was taken into account in determining the performance of Prob1 and Prob2 aptasensors in Hg^{2+} detection.

The Δ changes of Prob1 and Prob2 in various concentrations of Hg^{2+} solutions in the wavelength range of 400–1600 nm are given in Fig. 2. In the graph, 0 (zero) M curve was the measurements of the aptamer probe immobilized substrate obtained by spectroscopic ellipsometry. As seen in Fig. 2, after Hg^{2+} complex formation the Δ–λ relationship changed at all wavelengths. Besides, with the increase of Hg^{2+} concentration, sensor response for Prob1 and Prob2 differ from the bare chip surface but similar to Hg^{2+} retained surface, and almost parallel in all cases. Especially in the wavelength range of 600–700 nm, Δ–λ relationship was determined to be linear. Taking into account the change in this region, the Hg^{2+} detection performance of the aptasensor was determined with a spectroscopic ellipsometer.

The Δ–λ relationship between 600 and 700 nm gave a linear function with a regression coefficient (R^2) of around 0.98 at all concentrations. The Δ–λ lines in this wavelength range have shifted to higher Δ values but have had similar slopes with increasing Hg^{2+} concentration. To analyze the sensor response, the differences in this range Δ were taken into account and the differences were determined for 1 nM, 1 µM, 10 µM, 100 µM, 1 mM and 10 mM are given in Table 2.

The sensor response increased with increasing mercury concentration. As expected, the multiple site Hg^{2+} binding

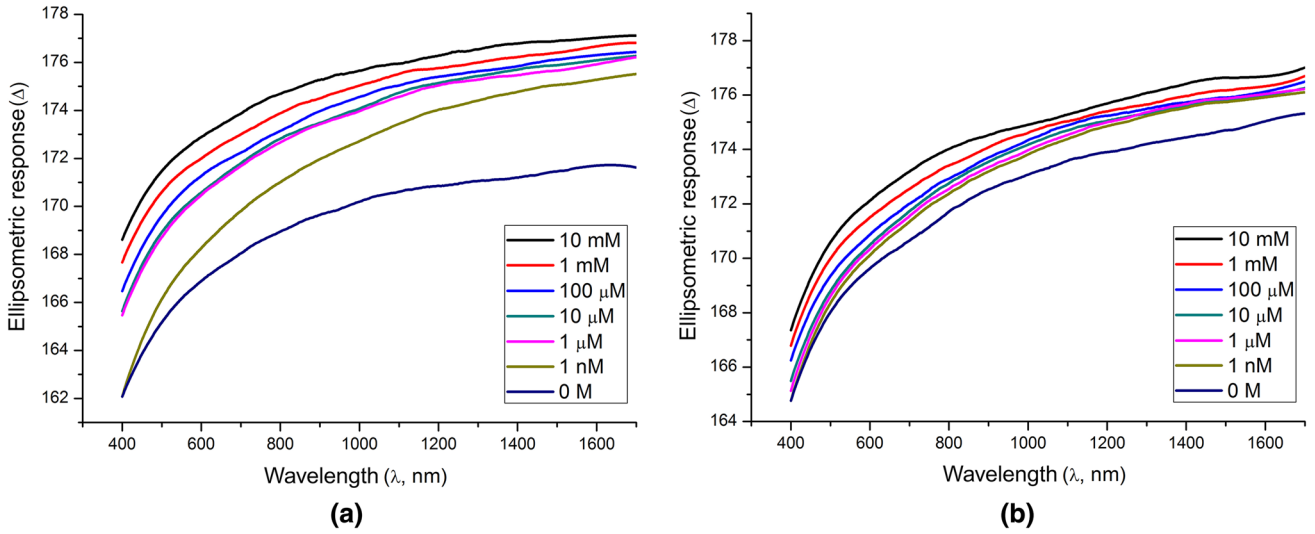

Fig. 2 Spectroscopic ellipsometry response (Δ change) for the **a** Prob1 and **b** Prob2

Table 2 Sensor response of Prob1 ve Prob2 for various mercuric ion concentrations and selectivity

Concentration (μM)	Prob1—sensor response (Δ, °)	Prob2—sensor response (Δ, °)
10,000	5.902 ± 0.044	2.515 ± 0.021
1000	5.041 ± 0.041	1.882 ± 0.019
100	4.306 ± 0.056	1.298 ± 0.036
10	3.714 ± 0.031	0.970 ± 0.067
1	3.610 ± 0.022	0.808 ± 0.056
0.01	1.581 ± 0.127	0.594 ± 0.063
1 μM Pb^{2+}	0.063 ± 0.042	0.081 ± 0.072
100 μM Pb^{2+}	0.089 ± 0.047	0.092 ± 0.061

of the aptasensor gives a logarithmically varying isotherm curve. This indicates that at low Hg^{2+} concentrations, the sensor response will be linear. Sensor calibration curves are given in Fig. 3. The sensing capacity of the sensor was high even at low concentrations. While the response of the sensor at a concentration of 1 nM was 1.58°, this response increased up to 5.9° at a concentration of 10 mM. The data obtained for the Prob2 sensor are also given in Table 2. It can be seen that the response for Prob2 aptasensor was more linear at higher Hg^{2+} concentrations. The sensor response between 1 nM and 10 μM concentrations ranged from 0.5° to 0.9°, up to 1.8° at 1 mM and 2.5° at 10 mM.

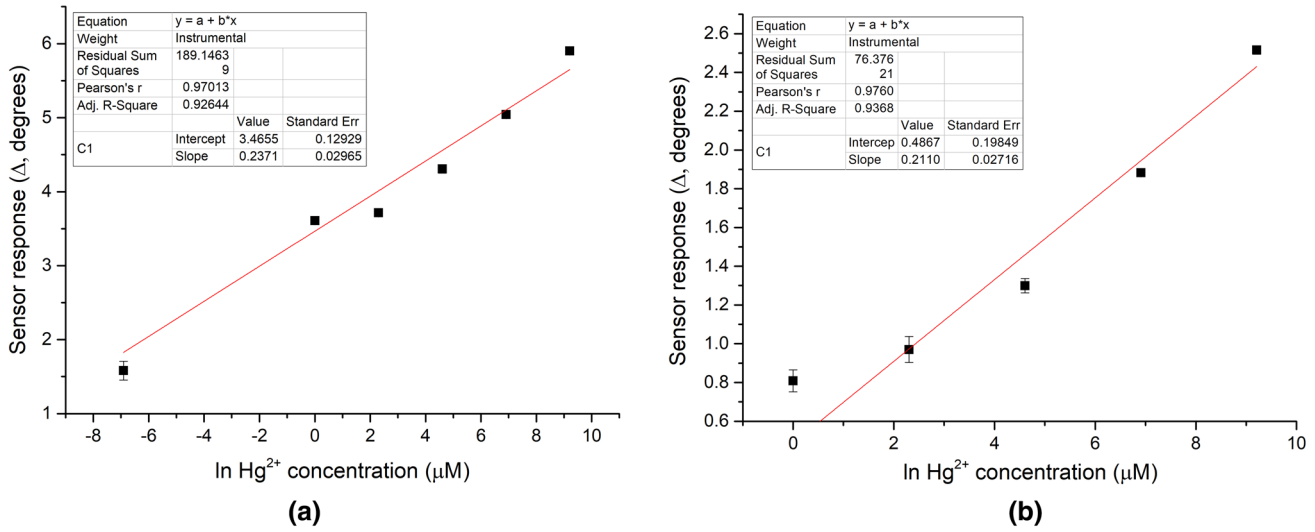

Fig. 3 Calibration curves for Prob1 (**a**) and Prob2 (**b**)

Table 2 also gives the results of the selectivity experiment with 1 µM Pb^{2+} and 100 µM Pb^{2+}. Although the specificity of aptamers (i.e. specificity of T–Hg^{+2}–T mismatch) is known and has been reported by various researchers, herein Pb^{2+} ions which are known as the most significant interferent was used for to show the specificity of the sensor (Farzin et al. 2015; Li et al. 2010; Wordofa et al. 2016; Wu et al. 2020). As can be seen from Table 2, the response of the aptasensor obtained as a result of selectivity experiments remained within the noise limits.

Sensor linearity and detection limit are important in sensor applications rather than kinetic change. The log Hg^{2+} concentration–sensor response (Δ) graph was drawn to evaluate the sensor performance of the Prob1 and Prob2 (Fig. 3.). This graph was used to determine the sensor detection limit and gave the first-order linear function of $y = ax + b$ ($R^2 = 0.98$ for Prob1 and $R^2 = 0.94$ for Prob2). As seen in Fig. 3, the aptasensor gives a semi-log concentration–sensor response curve and exhibits a kinetical behavior between aptamer and Hg^{2+}. The detection limit calculated on this DNA-aptasensor, called Prob1, is 0.89 pM (3σ S/N ratio) and the detection sensitivity is 0.237°/µM (slope of the line). The detection limit calculated on the Prob2 DNA aptasensor is 187 nM and the detection sensitivity is 0.211 degrees/µM.

Conclusions

Experiments were carried out for DNA aptamers having a linear structure (Prob1) and hairpin structure (Prob2). While evaluating ellipsometric analysis, the phase shift (Δ) parameter was taken into consideration. Assuming that the reflection parameters for dielectric substances are directly dependent on the layer thickness for homogeneous layers, the accumulation on the surface as a result of hybridization was observed as the relative change of the Δ.

The noise, σ, as the standard deviation for both aptasensors was determined as 0.054° and 0.044°, respectively. When determining the LOD for the sensor, an uncertainty of 3σ was considered with the most aggressive approach. Taking this uncertainty into consideration, the detection limit calculated on the Prob1 sensor is 0.89 pM and the detection sensitivity was found to be 0.237°/µM. The detection limit calculated on the Prob2 sensor is 187 nM and the detection sensitivity was found to be 0.211°/µM. In the specificity study, the sensor response obtained with Pb^{2+} were 0.089 ± 0.047 (100 µM Pb^{2+}) and 0.063 ± 0.042 (1 µM Pb^{2+}) for Prob1, and 0.092 ± 0.061 (100 µM Pb^{2+}) and 0.081 ± 0.072 (1 µM Pb^{2+}) for Prob2. These responses are below the 3σ noise limit and show the specificity valid for the aptamer as stated in the literature. LOD value of Prob2 was within the detection limits encountered in the literature, and for Prob1, LOD was as low as 0.89 pM. Considering that the analyzes were carried out using 1 mL Hg^{2+} solutions, it can be said that the analytical performance of the proposed methods is satisfactory. The LOD values specified in the literature are slightly lower than the 1 ng/L (Approx. 5 pM) limit specified for the ultra-trace element detection standard. Also, the method is quite simple. The specified steps can be performed in a much shorter time and without advanced device usage knowledge, and the use of solution preparation and dilution steps. Consequently, two different aptasensors have been successfully used in the detection of ultra-trace amounts of Hg^{2+} from aqueous solutions using a spectroscopic ellipsometer, which is a highly sensitive optical detection method.

Acknowledgements The data of this study were obtained in 2014 as a graduate thesis of Engineer Tuğçe Ertan's at the Cumhuriyet University, Institute of Science, Department of Chemical Engineering. YOK Thesis Center Thesis Number is 374767. The authors would like to thank Cumhuriyet University Faculty of Engineering Deanery and Nanotechnology Engineering Department for providing laboratory facilities during the thesis studies. Also, the authors would kindly acknowledge Cumhuriyet University Scientific Research Projects Supporting Department (CUBAP) for their financial supports under project No: M565.

References

Abdi MM, Abdullah LC, Sadrolhosseini AR, Mat Yunus WM, Moksin MM, Tahir PM (2011) Surface plasmon resonance sensing detection of mercury and lead ions based on conducting polymer composite. PLoS ONE 6:e24578–e24578. https://doi.org/10.1371/journal.pone.0024578

Arwin H (2001) Is ellipsometry suitable for sensor applications? Sens Actuators A 92:43–51. https://doi.org/10.1016/S0924-4247(01)00538-6

Bacon JR, Butler OT, Cairns WRL, Cook JM, Davidson CM, Cavoura O, Mertz-Kraus R (2020) Atomic spectrometry update-a review of advances in environmental analysis. J Anal Atom Spectrom 35:9–53. https://doi.org/10.1039/c9ja90060h

Bareiß M et al (2012) Ultra-thin titanium oxide. Appl Phys Lett 101:083113. https://doi.org/10.1063/1.4745651

Caglayan MO, Üstündağ Z (2020) Spectrophotometric ellipsometry based Tat-protein RNA-aptasensor for HIV-1 diagnosis. Spectrochimica Acta Part A 227:117748. https://doi.org/10.1016/j.saa.2019.117748

Caglayan MO, Sayar F, Demirel G, Garipcan B, Otman B, Celen B, Piskin E (2009) Stepwise formation approach to improve ellipsometric biosensor response. Nanomedicine 5:152–161. https://doi.org/10.1016/j.nano.2008.12.006

Chah S, Yi J, Zare RN (2004) Surface plasmon resonance analysis of aqueous mercuric ions. Sens Actuat B 99:216–222. https://doi.org/10.1016/j.snb.2003.11.015

Chamier J, Crouch AM (2012) Improved photoelectrochemical detection of mercury (II) with a TiO_2-modified composite photoelectrode. Mater Chem Phys 132:10–16. https://doi.org/10.1016/j.matchemphys.2011.06.041

Chang CC, Lin S, Wei SC, Chen CY, Lin CW (2011) An amplified surface plasmon resonance "turn-on" sensor for mercury ion using gold nanoparticles. Biosens Bioelectron 30:235–240. https://doi.org/10.1016/j.bios.2011.09.018

Chao C-H et al (2012) A rapid and portable sensor based on protein-modified gold nanoparticle probes and lateral flow assay for naked eye detection of mercury ion. Microelectron Eng 97:294–296. https://doi.org/10.1016/j.mee.2012.03.015

Chen C, Wang J (2020) Optical biosensors: an exhaustive and comprehensive review. Analyst 145:1605–1628. https://doi.org/10.1039/C9AN01998G

Chen Y, Yang C, Yu Z, Chen B, Han Y (2015) A highly sensitive hemicyanine-based fluorescent chemodosimeter for mercury ions in aqueous solution and living cells. RSC Adv 5:82531–82534. https://doi.org/10.1039/c5ra13802g

Clarkson TW, Magos L (2006) The toxicology of mercury and its chemical compounds. Crit Rev Toxicol 36:609–662. https://doi.org/10.1080/10408440600845619

Clarkson TW, Magos L, Myers GJ (2003) The toxicology of mercury–current exposures and clinical manifestations. N Engl J Med 349:1731–1737. https://doi.org/10.1056/NEJMra022471

Dalmieda J, Kruse P (2019) Metal cation detection in drinking water. Sensors (Switzerland). https://doi.org/10.3390/s19235134

Demirel G, Çağlayan MO, Garipcan B, Duman M, Pişkin E (2007a) Formation and organization of amino terminated self-assembled layers on Si(001) surface. Nanoscale Res Lett 2:350. https://doi.org/10.1007/s11671-007-9071-7

Demirel G, Çağlayan MO, Garipcan B, Duman M, Pişkin E (2007b) Oriented immobilization of IgG on hydroxylated Si(001) surfaces via protein-A by a multiple-step process based on a self-assembly approach. J Mater Sci 42:9402–9408. https://doi.org/10.1007/s10853-007-1809-1

Dragone R, Frazzoli C, Grappelli C, Campanella L (2009) A new respirometric endpoint-based biosensor to assess the relative toxicity of chemicals on immobilized human cells. Ecotoxicol Environ Saf 72:273–279. https://doi.org/10.1016/j.ecoenv.2008.02.011

Ellington AD, Szostak JW (1990) vitro selection of RNA molecules that bind specific ligands. Nature 346:818–822. https://doi.org/10.1038/346818a0

Ellington AD, Szostak JW (1992) Selection in vitro of single-stranded DNA molecules that fold into specific ligand-binding structures. Nature 355:850–852. https://doi.org/10.1038/355850a0

Fang SJ, Chen W, Yamanaka T, Helms CR (1996) Comparison of Si surface roughness measured by atomic force microscopy and ellipsometry. Appl Phys Lett 68:2837–2839. https://doi.org/10.1063/1.116341

Fanous A, Weiss W, Gorg A, Jacob F, Parlar H (2008) A proteome analysis of the cadmium and mercury response in *Corynebacterium glutamicum*. Proteomics 8:4976–4986. https://doi.org/10.1002/pmic.200800165

Farzin L, Shamsipur M, Tabrizi MA (2015) Biomagnetic separation and pre-concentration of trace amounts of Hg^{2+} in biological samples based on T-rich oligonucleotide modified magnetic beads. Anal Methods 7:8947–8953. https://doi.org/10.1039/C5AY01827G

Fen YW, Mat Yunus WM, Moksin M, Talib Z, Yusof N (2011) Surface plasmon resonance optical sensor for mercury ion detection by crosslinked chitosan thin film. J Optoelectron Adv Mater 13:273–279

Gabr MT, Christopher Pigge F (2017) A turn-on AIE active fluorescent sensor for Hg^{2+} by combination of 1,1-bis(2-pyridyl)ethylene and thiophene/bithiophene fragments. Mater Chem Front. https://doi.org/10.1039/c7qm00085e

Grisci G, Mróz W, Catellani M, Kozma E, Galeotti F (2016) Off-on fluorescence response of a cysteine-based perylene diimide for mercury detection in water. ChemistrySelect 1:3033–3037. https://doi.org/10.1002/slct.201600614

Hermann T, Patel DJ (2000) Adaptive recognition by nucleic acid aptamers. Science 287:820–825. https://doi.org/10.1126/science.287.5454.820

Jayasena SD (1999) Aptamers: an emerging class of molecules that rival antibodies in diagnostics. Clin Chem 45:1628–1650

Jia J, Ling Y, Gao ZF, Lei JL, Luo HQ, Li NB (2015) A regenerative electrochemical biosensor for mercury(II) by using the insertion approach and dual-hairpin-based amplification. J Hazard Mater 295:63–69. https://doi.org/10.1016/j.jhazmat.2015.04.017

Jiang T, Ke B, Chen H, Wang W, Du L, Yang K, Li M (2016) Bioluminescent probe for detecting mercury(II) in living mice. Anal Chem 88:7462–7465. https://doi.org/10.1021/acs.analchem.6b02200

Jin G, Meng YH, Liu L, Niu Y, Chen S, Cai Q, Jiang TJ (2011) Development of biosensor based on imaging ellipsometry and biomedical applications. Thin Solid Films 519:2750–2757. https://doi.org/10.1016/j.tsf.2010.12.175

Lech T (2014) ICP OES and CV AAS in determination of mercury in an unusual fatal case of long-term exposure to elemental mercury in a teenager. Forensic Sci Int 237:e1–5. https://doi.org/10.1016/j.forsciint.2014.02.015

Li L, Li B, Qi Y, Jin Y (2009) Label-free aptamer-based colorimetric detection of mercury ions in aqueous media using unmodified gold nanoparticles as colorimetric probe. Anal Bioanal Chem 393:2051–2057. https://doi.org/10.1007/s00216-009-2640-0

Li Q, Zhou X, Xing D (2010) Rapid and highly sensitive detection of mercury ion (Hg^{2+}) by magnetic beads-based electrochemiluminescence assay. Biosens Bioelectron 26:859–862. https://doi.org/10.1016/j.bios.2010.07.098

Liu X, Cheng X, Bing T, Fang C, Shangguan D (2010) Visual detection of Hg^{2+} with high selectivity using thymine modified gold nanoparticles. Anal Sci 26:1169–1172. https://doi.org/10.2116/analsci.26.1169

Liu H, Ma L, Ma C, Du J, Wang M, Wang K (2016) Quencher-free fluorescence method for the detection of mercury(II) based on polymerase-aided photoinduced electron transfer strategy. Sensors (Basel). https://doi.org/10.3390/s16111945

Narukawa T, Iwai T, Chiba K, Feldmann J (2018) A method for methylmercury and inorganic mercury in biological samples using high performance liquid chromatography-inductively coupled plasma mass spectrometry. Anal Sci 34:1329–1334. https://doi.org/10.2116/analsci.18P255

Poksinski M, Arwin H (2003) situ monitoring of metal surfaces exposed to milk using total internal reflection ellipsometry. Sens Actuat B 94:247–252. https://doi.org/10.1016/S0925-4005(03)00382-4

Ramos E, Pineiro D, Soto M, Abanades DR, Martin ME, Salinas M, Gonzalez VM (2007) A DNA aptamer population specifically detects Leishmania infantum H2A antigen Laboratory investigation. J Tech Methods Pathol 87:409–416. https://doi.org/10.1038/labinvest.3700535

Tombelli S, Minunni M, Mascini M (2007) Aptamers-based assays for diagnostics, environmental and food analysis. Biomol Eng 24:191–200. https://doi.org/10.1016/j.bioeng.2007.03.003

Tompkins HG, Zhu T, Chen E (1998) Determining thickness of thin metal films with spectroscopic ellipsometry for applications in magnetic random-access memory. J Vac Sci Technol A 16:1297–1302. https://doi.org/10.1116/1.581277

Tuerk C, Gold L (1990) Systematic evolution of ligands by exponential enrichment: RNA ligands to bacteriophage T4 DNA polymerase. Science 249:505–510. https://doi.org/10.1126/science.2200121

Wang T, Ma K, Liu W, Jin G, Niu Y (2019) Total internal reflection imaging ellipsometry biosensor: its principle and applications. AIP Conf Proc 2110:020007. https://doi.org/10.1063/1.5110801

Wordofa DN, Ramnani P, Tran T-T, Mulchandani A (2016) An oligonucleotide-functionalized carbon nanotube chemiresistor for sensitive detection of mercury in saliva. Analyst 141:2756–2760. https://doi.org/10.1039/C6AN00018E

Wu S, Yu Q, He C, Duan N (2020) Colorimetric aptasensor for the detection of mercury based on signal intensification by rolling

circle amplification. Spectrochim Acta Part A 224:117387. https://doi.org/10.1016/j.saa.2019.117387

Xiao W, Xiao M, Fu Q, Yu S, Shen H, Bian H, Tang Y (2016) A portable smart-phone readout device for the detection of mercury contamination based on an aptamer-assay nanosensor. Sensors (Basel). https://doi.org/10.3390/s16111871

Yim C, O'Brien M, McEvoy N, Winters S, Mirza I, Lunney JG, Duesberg GS (2014) Investigation of the optical properties of MoS2 thin films using spectroscopic ellipsometry. Appl Phys Lett 104:103114. https://doi.org/10.1063/1.4868108

Zapata F, Caballero A, Molina P, Tarraga A (2010) A ferrocene-quinoxaline derivative as a highly selective probe for colorimetric and redox sensing of toxic mercury(II) cations. Sensors (Basel) 10:11311–11321. https://doi.org/10.3390/s101211311

Zhang Y, Lai BS, Juhas M (2019) Recent advances in aptamer discovery and applications. Molecules (Basel, Switzerland) 24:941. https://doi.org/10.3390/molecules24050941

Zuker M (2003) Mfold web server for nucleic acid folding and hybridization prediction. Nucleic Acids Res 31:3406–3415. https://doi.org/10.1093/nar/gkg595